ELSEVIER

Contents lists available at ScienceDirect

## **Quaternary Science Reviews**

journal homepage: www.elsevier.com/locate/quascirev



# Late-Holocene hydroclimate inferences for the northern Great Basin from Little Lake, Elko County, Nevada, USA



Jeffrey S. Munroe

Geology Department, Middlebury College, Middlebury, VT, 05753, USA

#### ARTICLE INFO

Article history:
Received 8 May 2020
Received in revised form
13 July 2020
Accepted 19 July 2020
Available online 6 August 2020

Keywords: Hydroclimate Holocene Nevada Great basin Dunes

#### ABSTRACT

Prominent lunette dunes 500-800 m long, 50-80 m wide, and up to 5 m tall are present on the floor of the Independence Valley in northeast Nevada, USA. These dunes border the downwind margins of circular playas at the end of a drainage descending from the East Humboldt Mountains, which terminates in an ephemeral water body named Little Lake. Gastropod shells from the Little Lake playa yield radiocarbon ages of ~400 cal yr BP, after correction for a hard-water effect. A similar age was obtained for shells from the crest of one of the lunettes. Deeper sediment in this lunette yielded shell ages clustering around 600 cal yr BP. This pattern suggests two intervals of relatively persistent water at Little Lake, both of which ended with lake desiccation and deflation of sediment and shells to the adjacent lunette. Shells from the crest of another lunette yielded radiocarbon ages between 3800 and 1750 cal yr BP. This dune, therefore, is considerably older and accumulated over a much longer stretch of time. Using the Global Surface Water Explorer, years between 1984 and 2018 were identified in which Little Lake contained water in most of the available summer imagery. These years form three clusters: 1984-1987, 1997-2000, and 2017-2018. Snow water equivalent (SWE) is greater in the mountains, snow makes up a greater percent of total annual precipitation, and Palmer Drought Severity Index is more positive in this region, in years when water is present in Little Lake compared with those in which the lake remains dry. Values of the PDO are also higher in years when Little Lake holds water. Although the hydrology of Little Lake may be influenced to an unknown degree by upstream water diversions, this overall pattern implies that the lake and its associated lunettes are a sensitive recorder of late Holocene hydroclimate variability in the northern Great Basin.

© 2020 Elsevier Ltd. All rights reserved.

## 1. Introduction

The vast internally drained region known as the Great Basin is the most arid part of North America. Owing to the rain shadow induced by the Sierra Nevada mountain range to the west, precipitation across this region is minimal (Poage and Chamberlain, 2002). Normal faulting in response to crustal extension beginning in the middle Miocene (Long, 2019) has produced a Basin and Range landscape, with locally extreme gradients in topography, climate, and the corresponding distribution of flora and fauna (Grayson, 2011). By virtue of their hydrologic closure, lower elevations within the Great Basin hosted extensive lakes during wetter "pluvial" episodes of the Pleistocene (Mifflin and Wheat, 1979; Reheis, 1999a). Geomorphic features and accumulations of lacustrine sediment produced by these lakes have provided a wealth of

information about hydroclimate changes over glacial-interglacial cycles (e.g. Adams and Wesnousky, 1998; Bacon et al., 2006; Benson et al., 2011; Munroe and Laabs, 2013a; Reheis, 1999b; Zimmerman et al., 2011). Most of these lakes, however, desiccated and disappeared entirely as the Pleistocene came to an end (Steponaitis et al., 2015), meaning that their deposits are of limited utility for studying Holocene hydroclimate change. Moisture sensitive tree ring records are useful on Holocene timescales, and although the landscape of the Great Basin is not extensively forested, the region is fortunately home to several tree species which are notably long-lived (Salzer et al., 2014). Springfed wetlands have yielded important information from pollen, diatoms, and other biological proxies (Louderback and Rhode, 2009; Mensing et al., 2013). Similarly, sediments obtained from existing lakes in glaciated landscapes at the highest elevations have provided records about how mountain ecosystems evolved during the postglacial period (Munroe et al., 2018; Reinemann et al., 2014, 2009; Wahl et al., 2015). As a result, it is clear that the climate of this region varied considerably after the late Pleistocene pluvial maximum, yet numerous questions remain.

An additional source of paleoclimate information, with the potential to connect the mountains and the intervening basins at lower elevation, is isolated lakes fed by runoff from the high mountains (Adams and Rhodes, 2019). Some of these lakes are permanent, whereas others are ephemeral. In all cases, the volume of these lakes fluctuates in response to climatic shifts that impact the balance between inflowing water and evaporation (Benson and Paillet, 1989). As a result, shorelines constructed by these lakes at various elevations (Hatchett et al., 2015), and changes in their chemistry as recorded in sediments and biologic remains (Benson et al., 2002), can be used to reconstruct past hydroclimate variations. In extreme cases, these lakes disappear and refill in response to high-amplitude variations in effective moisture, leading to the formation of dunes that are indirect evidence for the former presence or absence of surface water (Munroe et al., 2017).

Despite commanding aridity, the Great Basin hosts some of the larger and most rapidly growing cities in North America (Frey, 2012). Water is also artificially diverted from the Great Basin and delivered to major urban areas in southern California (Wiens et al., 1993). As a result, millions of people are reliant upon the relatively meager surface water resources of this area, and are correspondingly vulnerable to hydroclimate changes in the future (Cayan et al., 2010; Karl and Melillo, 2009). This concern is particularly relevant given numerical modeling experiments suggesting that aridity in already arid regions will increase in the future as a result of climatic shifts induced by rising greenhouse gas concentrations (Held and Soden, 2006). Accurately predicting future water availability, and designing effective management plans for dealing with future water shortages, are major challenges for water resource managers, civil engineers, urban planners, and others involved in making decisions that will impact this region for decades to come.

This multi-phase project developed a hydroclimate record spanning the last several thousand years from a small terminal basin in northeastern Nevada. The basin receives runoff from the highest mountains in the internal Great Basin, which serve as the

headwaters for the Humboldt River, the longest river system in the region. In the first phase, climate data from the past few decades were combined with satellite imagery to determine the climatic conditions under which a lake is present in this terminal basin. In the second phase, a combination of sedimentological and geochronological techniques was directed at prominent dunes standing on the downwind border of the lake basin, dunes which presumably formed at times when the lake desiccated. Finally, results were compared with a composite of moisture-sensitive treerings and other paleoclimate records to reconstruct the hydroclimate of this site over the past ~4000 years. Because this lake serves as a distal recorder of hydroclimate conditions in a mountain range that is the source of a regionally extensive river system, results of this study have significance across the northern Great Basin, and provide an improved understanding of the timing and magnitude of climatic changes in this region over the past several thousand years.

## 2. Setting

The study area for this project is the Independence Valley of northeastern Nevada, USA (Fig. 1). The Independence Valley, together with the adjacent Clover Valley, form a broad lowland, ~35 km wide, between the Pequop Mountains to the east and the East Humboldt Mountains to the west (Fig. 1). Maximum elevations in the Pequop Mountains reach ~2800 m, whereas the East Humboldt Mountains are higher, reaching ~3450 m. The East Humboldt Mountains contain abundant evidence for past glacial activity in the form of erosional features like cirques and striated bedrock, and depositional landforms including moraines and outwash (Laabs et al., 2013). The area around Angel Lake in the northeastern part of the East Humboldt Mountains was designated as the type locality for the last major glaciation in the Great Basin, which is correspondingly known as the Angel Lake Glaciation (Sharp, 1938). Cosmogenic surface-exposure dating indicates that this glaciation reached its maximum extent around 18,000 years ago, and glaciers were likely absent from the East Humboldt Mountains after

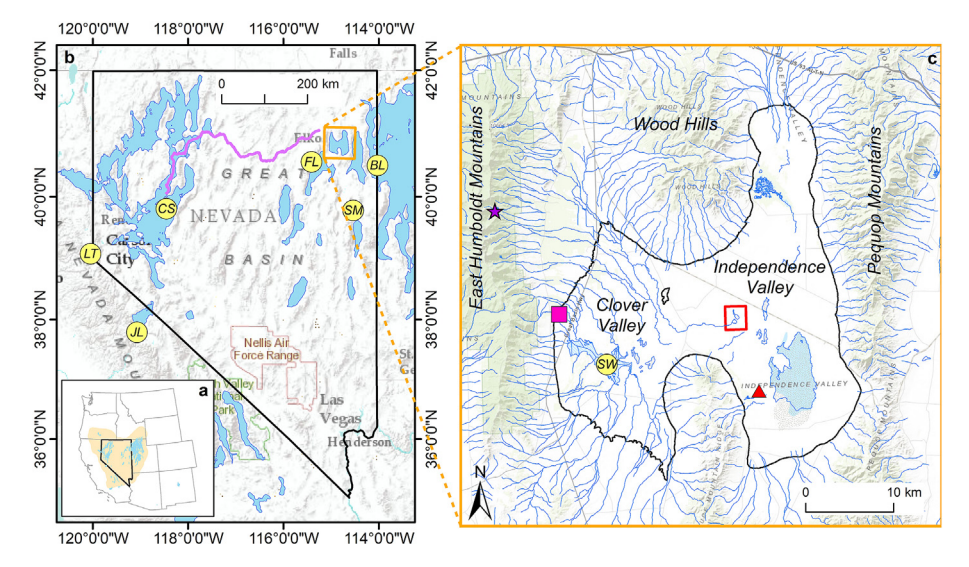


Fig. 1. (a) Inset map showing the state of Nevada (bold outline) in the western US. The beige polygon delineates the Great Basin, and blue polygons represent pluvial lakes [7]; (b) Enlarged view of Nevada and pluvial lakes during the late Pleistocene. The purple line is the Humboldt River extending from the East Humboldt Mountains (east) to the Carson Sink (CS). Locations mentioned in the text are identified, including Blue Lake (BL), Favre Lake (FL), Stonehouse Meadow (SM), Lake Tahoe and Fallen Leaf Lake (IT), and June Lake (JL). The orange square highlights Lake Clover and represents the area of panel c; (c) Enlargement of the Clover and Independence Valleys. The extent of Lake Clover at its highstand is outlined in black. The red box highlights the Little Lake area in Fig. 2. The red triangle marks the location of the grid node in the interpolated Living Blended Drought Atlas (Cook et al., 2010). The purple star marks the location of the Hole in Mountain SNOTEL site in the East Humboldt Mountains. The pink square denotes National Weather Service site 261740 in the Clover Valley. Snow Water Lake is identified as SW. Stream systems, most of which are ephemeral, are shown in blue.

approximately 14,000 years ago (Munroe et al., 2018).

In contrast to the elevations attained by the mountains, the floor of the Independence and Clover Valleys has a low point of ~1700 m. Areas below 1725 m were inundated in the late Pleistocene by a water body known as pluvial Lake Clover (Mifflin and Wheat, 1979). This lake reached its maximum surface area of 740 km² around 16,000 years ago (Munroe et al., 2020), overlapping with the glacial maximum in the mountains to the west (Munroe and Laabs, 2013b). Application of radiocarbon and luminescence dating reveals that Lake Clover regressed from its highstand over several thousand years, and that the youngest identifiable beach ridges were built in the earliest Holocene (Munroe et al., 2020).

Since the final regression of Lake Clover, surface water at the lowest elevations has been focused in just a few locations. One of these is Snow Water Lake on the floor of the Clover Valley (Fig. 1), which is fed by snowmelt and runoff from the southern part of the East Humboldt Mountains (Munroe et al., 2017).

In contrast, streams descending eastward from the northern part of the East Humboldt Mountains, as well as from the southwestern part of the lower Wood Hills, converge as a single waterway that skirts Snow Water Lake to the northeast (Fig. 1), passes through the saddle connecting the Clover and Independence Valleys, and terminates in a pair of interconnected basins known as Little Lake (Fig. 2). Both of these basins are nearly circular with a diameter of ~400 m and have unvegetated floors of cracked silty clay. Notably, Little Lake is bordered on the east by a pair of crescentic "lunette" dunes ~800 m long, 100 m wide, and ~5 m tall. These lunettes are conspicuous on aerial photos and topographic maps (Fig. 2). Several additional lunettes of similar scale, but more muted form, are present within 2 km to the southeast of Little Lake (Fig. 2). None of these are connected to the modern drainage system.

The climate of the Little Lake area can be approximated by conditions measured at NWS cooperative site 261740 (Fig. 1) at the

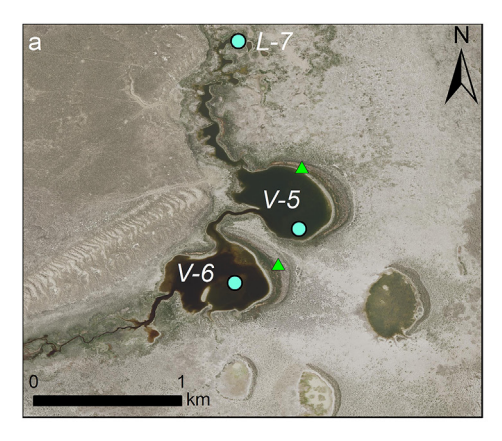
foot of the East Humboldt Mountains (20 km west and 50 m higher in elevation), where the mean annual air temperature is 7.5 °C and mean annual precipitation is 350 mm. Mean monthly air temperatures peak in July (29.7 °C), and are lowest in January (2.6 °C). July and August are both very dry averaging <16 mm of precipitation. January has the greatest average precipitation (45 mm), followed by November, December, and February (~38 mm). Spring months average ~30 mm of precipitation. Wind data are available for Elko, NV ~80 km to the west where mean monthly windspeeds are highest in in the spring, reaching a maximum of 3.2 m/s in April. December has the slowest mean windspeed (2.2 m/s). Wind directions are dominantly from the west between March and October and from the east in the winter.

#### 3. Methods

#### 3.1. Climatic conditions

Precipitation over the past several decades in the headwaters of the drainages leading to Little Lake was constrained by data collected at the Hole in Mountain SNOTEL (snowpack telemetry) site. This SNOTEL station is perched at the lip of a prominent cirque on the eastern side of the East Humboldt Mountains at an elevation of 2488 m (Fig. 1). Daily data for cumulative precipitation and snow water equivalent (SWE) were downloaded for October 1, 1981 through September 30, 2018.

General climate data for the region surrounding Little Lake were downloaded from the National Oceanographic and Atmospheric Administration <a href="https://www.nesdis.noaa.gov/">https://www.nesdis.noaa.gov/</a>. Data for precipitation, temperature, and various drought metrics were downloaded for January, 1983 through January, 2019 for the Northeastern division (02) of Nevada. A time-series of the Pacific Decadal Oscillation (PDO) from 1948 through 2018 was also downloaded from the National Oceanographic and Atmospheric Administration Physical



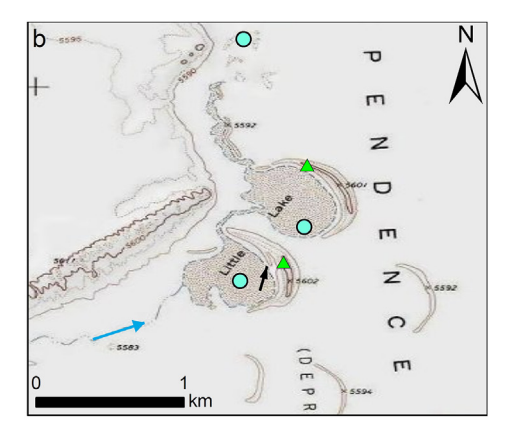




**Fig. 2.** (a) True color aerial photo (National Aerial Photography Program) of Little Lake showing the flooded VEN-5 (V-5) and VEN-6 (V-6) basins, along with the L-7 site at the ultimate downstream end of the drainage. Blue circles mark the locations where shells were collected from the playa surface. Green triangles mark the locations of the auger holes into the crest of the VEN-5 and VEN-6 dunes; (b) a portion of the USGS 7.5' Ventosa quadrangle showing the same location as panel (a). The blue arrow notes the flow direction of the stream system delivering water to Little Lake. The black arrow highlights the inset dune ridge at VEN-6. In both panels, note the presence of additional lunettes to the southeast of Little Lake that are not connected with the modern stream system; (c) a panoramic composite of photographs presenting the view southward from the dune crest at VEN-5 over the dry floor of Little Lake in June, 2019. The East Humboldt Mountains are visible to the right, with the snow covered Ruby Mountains farther away to the southwest.

Science Laboratory <a href="https://psl.noaa.gov/enso/dashboard.html">https://psl.noaa.gov/enso/dashboard.html</a>. Monthly average data were used to calculate summary statistics on water year (WY) intervals (October, 1 through September, 30).

The paleohydrology of the Little Lake watershed is constrained by a gridded composite  $(0.5^\circ)$  of moisture-sensitive tree-ring records known as the Living Blended Drought Atlas-LBDA (Cook et al., 2010). A grid point within the LBDA is located immediately south of Little Lake (40.75° N, 114.75° W) on the floor of the Independence Valley (Fig. 1); the data for this point, the center of a cell (~2300 km²) covering the East Humboldt and Pequop Mountains, are considered to represent overall drought conditions in the Little Lake watershed. The LBDA was queried for reconstructed values of the Palmer Drought Severity Index (PDSI) spanning the past ~2000 years.

Satellite imagery and aerial photos reveal that Little Lake was present on the floor of the Independence Valley occasionally over the last several decades (Fig. 3). To explore the climatic conditions corresponding with the presence of surface water at this location, the Global Surface Water Explorer (GSWE) <a href="https://global-surface-">https://global-surface-</a> water.appspot.com/> was queried to identify years in which water was present. The GSWE uses an extensive library of remotely sensed data to track the presence or absence of water at specific positions on the Earth's terrestrial surface. These observations are integrated monthly, as well as annually, to yield time-series of water occurrence. For the location of Little Lake, data are available from 1984 through 2018. The presence of water at Little Lake in these years was classified as "permanent", "seasonal", or "none", based on the fraction of months in which water was present out of the total number of available observations for that year. Statistical analysis using a non-parametric Kruskal-Wallis test was conducted to determine the significance of differences between average values of precipitation, April 1 SWE, and annual maximum SWE at the Hole in Mountain SNOTEL for these three classes of water occurrence. This same analysis was repeated for values of the PDSI and average temperature in the northeastern Nevada region, as well as for the PDO.

## 3.2. Field and labwork

During initial reconnaissance at Little Lake in August, 2018, abundant gastropod shells were noticed on the dry, mud-cracked playa surface (Fig. 4). Shells were also encountered within two hand excavations (VEN-5 and VEN-6) into the crest of the lunettes east of Little Lake (Fig. 2). Additional shells were collected from the same sites during a second visit in March, 2019, along with shells from the ultimate end of the drainage a short distance north of Little Lake (L-7, Fig. 2). A projectile point was also noted and photographed on the surface of the playa west of VEN-6 (Fig. 4). During a third field visit in June, 2019 a bucket auger was used to retrieve samples to a depth of 300 cm below the dune crest at VEN-5 and VEN-6. Sediment samples were collected every 50 cm and material from various depths was passed through a 2-mm sieve to isolate shells for radiocarbon dating. During this field visit an additional sampling site was established, VEN-6b, on a lower dune ridge inset to the main lunette just west of the VEN-6 site (Fig. 2, arrow). Finally, an exhaustive search for modern gastropods in the waterfilled reaches of the drainage leading to Little Lake, approximately 10 km upstream, was conducted in the hope of finding live snails that could be used to constrain any hard-water effect in the Little Lake hydrologic system. No living snails were found, but a sample of stream water was collected.

In the laboratory, sediment samples were processed for grain size analysis by deflocculation ( $\geq 3$  days) in sodium hexametaphosphate, followed by sonification and mixing. The resulting dispersed samples were analyzed with laser scattering in a Horiba







**Fig. 3.** Three views of Little Lake from Google Earth imagery showing a dry playa system in the fall of 2013, and partially flooded conditions in 2006 and 1999. In both of the latter cases, the tendency of the downstream VEN-5 playa to flood completely while the upstream VEN-6 playa remains partially emerged is obvious.

LA-950. This instrument reports grain size distribution on a volume basis and has an effective range from 50 nm to 3 mm. A refractive index of 1.54 with an imaginary component of 0.1i was used for calculations. Duplicates were run on all samples.

The geochemistry of sediment samples was constrained with X-ray fluorescence (XRF). In preparation for analysis, samples were ground to a fine powder in a shatterbox (1 min), and ignited at 1000 °C in a Leco TGA-701 thermogravimetric analyzer. After ignition, samples were crushed with a mortar and pestle and added to a borate flux (66.67% Li $_2$ B $_4$ O $_7$  - 32.83% LiBO $_2$  - 0.50% LiI) in a platinum crucible. This mixture was then heated to 1065 °C for 20 min in a Le Neo Fluxer to produce a glass disk that was analyzed for major elements on a Thermo ARL Quant'X EDXRF. Results were calibrated with the USGS Glass Mountain Rhyolite (RGM-1)

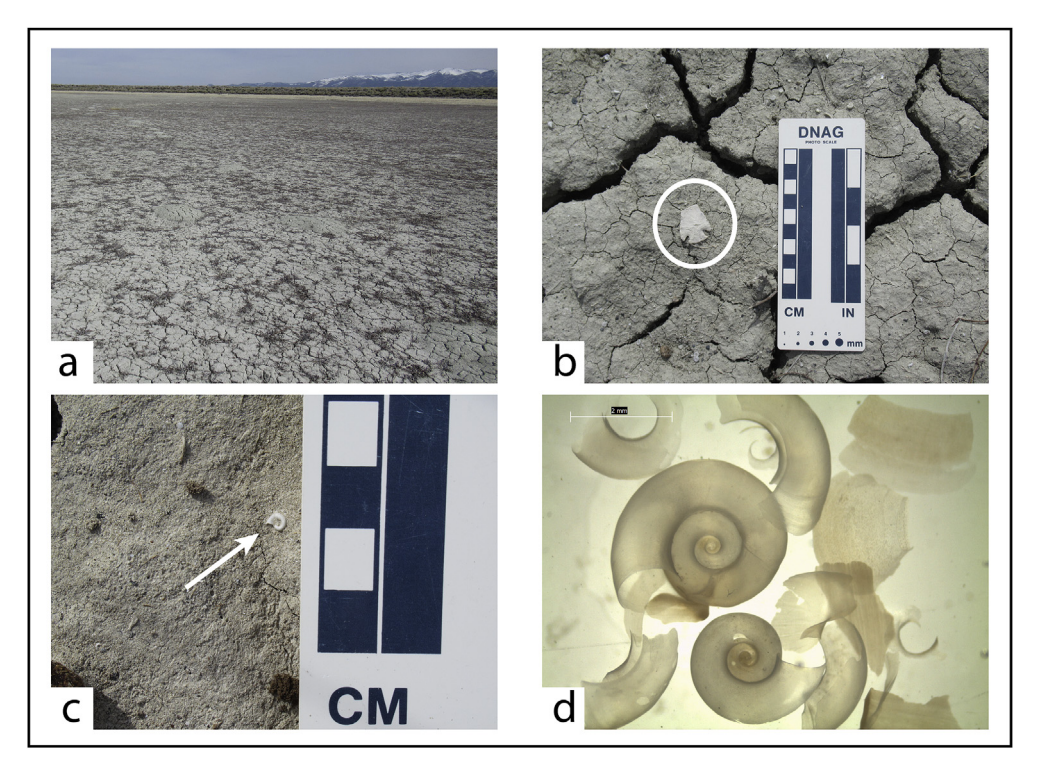


Fig. 4. (a) A representative photograph of the dry, sparsely vegetated, mud-cracked surface of the Little Lake playa in March, 2019; (b) a Rosegate Series projectile point (circled) noted on the surface of the playa; (c) A representative photograph of the gastropod shells (arrow) that are abundant on the playa surface; (d) Gastropod shells after sonication and HCl treatment prior to submission for radiocarbon dating. The scale bar in the upper left is 2 mm.

standard, which was made into a glass disk in the same manner as samples.

Mineralogical composition of the dune samples was determined through XRD analysis on bulk samples. Samples were run as random powders in a Bruker D8 diffractometer with CuK $\alpha$  radiation and a theta-theta goniometer. Scans extended from 2 to 50° 2 $\theta$  and proceeded at 3°/min. Analysis of XRD patterns using the software Eva permitted the identification of major mineral components. Quartz was represented by its 100 peak at 4.26 Å, plagioclase (002 at 3.18 Å), and calcite (100 at 3.03 Å).

In preparation for radiocarbon dating, gastropod shells were isolated from the sediment through a combination of wet sieving and picking beneath a binocular microscope. Shells were cleaned in distilled water through sonication, and secondary carbonate coatings were removed with a quick treatment with dilute (3%) HCl (Fig. 4). Shells were photographed under transmitted light and submitted to commercial laboratories (International Chemical Analysis – ICA and the National Ocean Sciences Accelerator Mass Spectrometry facility – NOSAMS) for AMS <sup>14</sup>C analysis. The water sample was also submitted to ICA for dating of dissolved inorganic carbon. This result is considered a maximum estimate for the possible hard-water effect in the Little Lake system. Accordingly, the radiocarbon age of this water sample was subtracted from the reported radiocarbon ages for the gastropod samples. Resulting corrected ages were calibrated using the IntCal13 calibration curve (Reimer et al., 2013) within OxCal 4.3 (Ramsey, 2006).

## 4. Results

## 4.1. Climate

Although Little Lake was dry during each of the three field visits (Fig. 4), imagery available in Google Earth clearly reveals that the

playa was flooded at times during the past several decades (Fig. 3). Analysis within the Global Surface Water Explorer database allows classification of the years between 1984 and 2018 in terms of how often Little Lake was present (Table 1). For 8 years (23%) water is classified as "permanent", meaning that water was observed in greater than 80% of the available imagery (Fig. 5). In an additional 9 years (25%), water is classified as seasonal, meaning that it was present in less than 50% of the available imagery. For 18 of the years (52%) no water was observed. The years of permanent water are grouped in three clusters: 1984 to 1987, 1997 to 1999, and 2017 (Fig. 5). Years of seasonal water bracket the second and third cluster, and additional isolated years of seasonal water are scattered between 2004 and 2015 (Table 1).

The Hole in the Mountain SNOTEL (Fig. 1, Table 1) received an average of 888 mm of precipitation per water year between 1984 and 2018 (range from 516 in WY 1987, to 1427 mm in WY 1984, Fig. 5). April 1 snow water equivalent (SWE) averaged 422 mm (range from 135 in WY 2015, to 991 mm in WY 1984). April 1 SWE comprised 15–85% of annual precipitation, with a mean of 46%. Maximum annual SWE averaged 487 mm. Temperature for the northeastern Nevada region averaged 7.8 °C (range from 6.3 °C in WY 1993 to 9.6 °C in WY 2016). The overall PDSI on a water year basis averaged –0.9, with a range from –5.0 (extreme drought, WY 2013) to +3.6 (severe wet, WY 1998). The PDO averaged 0.26 over this time interval.

The classification of individual water years in terms of water occurrence at Little Lake exhibits a strong correlation with estimated values of the local PDSI obtained from the LBDA (Fig. 5). The first cluster of years with permanent water from 1984 through 1987, and the second cluster between 1997 and 1999, both coincide with strongly positive values of the PDSI, indicating wet conditions. Values of the PDSI were again positive in 2017 when permanent water was noted. Years of seasonal water presence, for instance

**Table 1**Occurrence and climate data for little lake Nevada

Water Year	Months of Obs	Months with Water	Note	%	Code <sup>a</sup>	Precip <sup>b</sup>	Apr 1 SWE <sup>b</sup>	%	Max SWE <sup>b</sup>	Precip <sup>c</sup>	Temp <sup>c</sup>	PDSI <sup>c</sup>	PDO
	OI ODS	with water		_		mm	mm	_	mm	mm	С		
1984	2	2	Jun, Jul	100	P	1427	991	69	1300	483	6.8	6.8	0.97
1985	5	5	Apr, Jun—Sept	100	P	693	490	71	490	285	6.4	0.6	0.63
1986	7	7	Apr-Oct	100	P	_	_	_	521	353	7.8	0.4	0.85
1987	3	3	Apr, Jul and Aug	100	P	516	152	29	152	278	7.7	-2.4	1.86
1988	5	0	_	0	N	607	305	50	325	302	7.7	-1.9	0.92
1989	5	0	_	0	N	970	729	75	798	298	7.5	-2.0	-0.16
1990	5	0	_	0	N	673	338	50	358	292	8.0	-2.9	-0.04
1991	5	0	_	0	N	683	206	30	224	289	7.0	-3.3	-0.89
1992	6	0	_	0	N	587	142	24	203	246	8.6	-3.8	0.81
1993	4	0	_	0	N	1016	709	70	798	351	6.3	0.6	1.31
1994	6	0	_	0	N	594	152	26	224	268	8.2	-2.1	0.58
1995	3	0	_	0	N	1212	414	34	439	450	7.0	2.1	0.19
1996	7	1	Mar	14	S	955	815	85	815	325	8.4	2.5	0.69
1997	6	5	May, Jul-Oct	83	P	1232	930	75	998	425	7.8	2.4	1.16
1998	8	8	Mar-Oct	100	P	1080	561	52	655	463	7.3	3.6	0.73
1999	7	7	Mar, May-Oct	100	P	892	452	51	561	315	7.2	3.1	-0.77
2000	8	4	Mar–Jun	50	S	726	500	69	508	268	9.0	-2.5	-0.97
2001	8	1	Mar	13	S	658	211	32	241	261	8.0	-3.4	-0.38
2002	7	1	Feb	14	S	777	394	51	427	262	7.8	-3.6	-0.41
2003	5	0	_	0	N	777	241	31	287	294	8.5	-3.8	1.17
2004	7	1	Mar	14	S	841	274	33	455	313	7.9	-2.4	0.56
2005	7	0	_	0	N	892	434	49	490	444	7.5	3.0	0.52
2006	6	3	Jun-Aug	50	S	1115	925	83	970	360	8.2	1.4	-0.02
2007	6	0	_	0	N	770	145	19	231	265	8.3	-3.0	0.05
2008	7	0	_	0	N	897	599	67	645	240	7.1	-3.7	-1.23
2009	7	0	_	0	N	986	279	28	338	353	8.1	-1.5	-0.93
2010	7	1	Oct	14	S	818	325	40	401	286	6.8	-0.4	-0.06
2011	7	0	_	0	N	1229	521	42	696	438	7.3	2.5	-1.03
2012	7	0	_	0	N	696	183	26	221	226	8.6	-3.1	-1.40
2013	8	0	_	0	N	663	145	22	190	267	8.1	-5.0	-0.56
2014	8	0	_	0	N	927	434	47	470	331	8.4	-4.3	0.54
2015	8	1	Oct	13	S	881	135	15	310	297	9.6	-4.4	1.83
2016	8	0	_	0	N	_	444	_	444	400	8.2	1.0	1.52
2017	9	9	Feb-Oct	100	P	1250	_	_	_	427	8.5	0.5	0.76
2018	7	3	Apr–Jun	43	S	1275	368	29	384	249	8.9	-2.4	0.19

<sup>&</sup>lt;sup>a</sup> P = permanent water, S = seasonal water, N = no water.

2006 and 2009, also correspond with wetter conditions according to the PDSI. In contrast, the majority of years in which no water was observed exhibit negative PDSI values corresponding with drought. A similar pattern is seen when comparing with total water year precipitation and with April 1 SWE at the Hole in Mountain SNOTEL (Fig. 5).

Box plots further emphasize the pattern of wetter conditions corresponding with the presence of water at Little Lake, and drier years corresponding with water absence (Fig. 6). Although the 3-way differences as determined by a Kruskal Wallis test are not all significant, there is a clear pattern of greater mean precipitation, greater April 1 SWE, and of April 1 SWE representing a greater percent of the total annual precipitation in years when Little Lake is permanent. The value of the PDO and the PDSI is also greater during years with permanent water. This difference is significant (P < 0.05) between years of permanent and seasonal or no water. In contrast, there is no significant difference or clear trend between mean temperature in years of contrasting water presence at Little Lake (Fig. 6).

## 4.2. Sedimentology

The sediment grain size distributions measured with laser scattering are notably consistent from top to bottom within the two auger holes (Fig. 7). All samples are dominated by silt (65.8–78.2% by volume) and classify as silt loam textures. Very fine silt (2–7  $\mu m)$  is the most abundant size fraction (on average 32% by volume), and

 $7~\mu m$  is the overall modal grain size. Clay-sized material (<2 μm) comprises 9.8-23.6%, whereas sand (>63 μm) is 5.0-18.6% by volume. There is no obvious downhole change in grain size distribution in the two auger holes (Fig. 7). Samples from VEN-6 tend to contain more coarse and fine sand than those from VEN-5, however this difference is not statistically significant (P=0.054). Similarly, the average (mean and median) grain size is greater at VEN-6, but the difference is not significant (P=0.094 to 0.152).

XRF analysis confirms the similarity between samples collected from the two dunes (Fig. 8). All samples are dominated by silica, with an elemental abundance from ~57 to 63%. Calcium is the second most abundant major element (14–21%) followed by aluminum (~10%). In both dunes, the sequence of major elements in order of decreasing abundance is Si > Ca > Al > Mg > Fe > K > Na > Mn~Ti ~ P. Mineralogical analysis with XRD indicates that samples are dominated by quartz, calcite, and plagioclase (Fig. 8). Illite and other dioctahedral clay minerals were also detected. As with the grain size analysis, there are no patterns of consistent differences between the two dunes, or with depth in the two auger holes.

## 4.3. Radiocarbon dating

To provide age control for the dunes at Little Lake, 16 samples of gastropod shells along with one sample of modern water were radiocarbon dated. The dissolved inorganic carbon in the water sample returned a radiocarbon age of  $360 \pm 30$  years (Table 2). This

b At Hole in Mountain SNOTEL.

<sup>&</sup>lt;sup>c</sup> Mean value for Northeastern division of Nevada <a href="https://www.nesdis.noaa.gov/">https://www.nesdis.noaa.gov/</a>

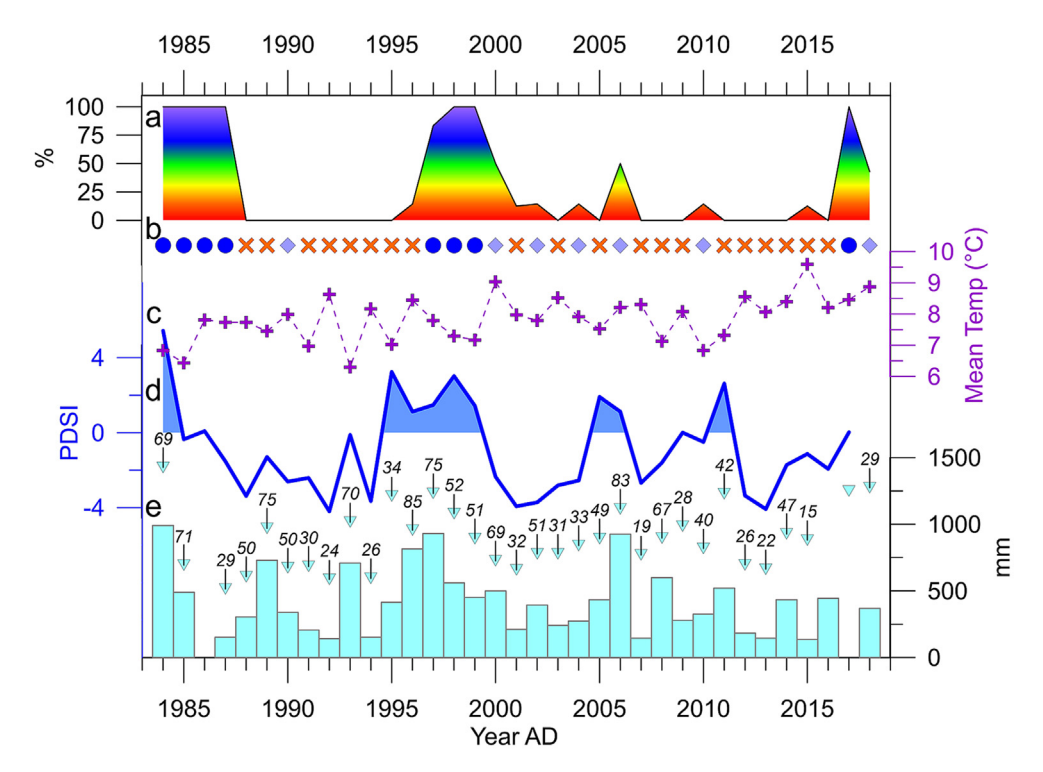


Fig. 5. (a) A time-series presenting the percentage of images available for the Little Lake region each year in which water was observed on the playa (Table 1), with redder color indicating lower percent and blue and purple hues corresponding to years in which Little Lake was permanent. (b) Years in which the presence of Little Lake was classified as permanent in the Global Surface Water Explorer are shown as blue circles. Years of seasonal water at Little Lake are shown in light blue diamonds, and years in which Little Lake failed to form are shown in orange crosses. (c) Mean annual temperature for northeastern Nevada shown as purple crosses. (d) The blue line presents the reconstructed Palmer Drought Sensitivity Index (PDSI) for the grid node in the Living Blended Drought Atlas (Cook et al., 2010) closest to Little Lake (Fig. 1). The time-series is filled above zero to highlight the correspondence of wet conditions with the presence of water at Little Lake. (e) The light blue bars present April 1 snow water equivalent (in mm) at the Hole in Mountain SNOTEL (Fig. 1). The blue triangles denote total water year precipitation, and the labels are the percent of total precipitation each year represented by the April 1 snowpack. Some years are missing data because of sensor malfunctions.

result indicates that considerable "old carbon" is present in the stream system leading toward Little Lake. Although not conclusive, this situation strongly suggests that aquatic gastropods living in this water would have artificially old radiocarbon ages. Therefore, 360 radiocarbon years were subtracted from the reported age of each of the gastropod samples before calibration. This approach is conservative, and may result in ages that have been adjusted to be "too young". However, in the absence of living, modern gastropods for which the radiocarbon offset could be directly determined, this approach is justified.

The gastropod shells collected from the modern playa surface at Little Lake (VEN-5 and VEN-6), as well as downstream at the ultimate termination of the drainage (L-7, Fig. 2) returned radiocarbon ages between 600 and 700 years BP (Table 2). After adjusting for the possible hard-water effect, these ages correspond to 300–400 cal yr BP (Fig. 9). In addition, the sample from 50 cm below the surface of the dune at VEN-5 yielded an identical result. Five additional samples collected at progressively greater depths within the auger hole at VEN-5 yielded a second group of ages that calibrate to between 500 and 600 cal yr BP (Fig. 9). Thus it appears that the VEN-5 dune was constructed between 600 and 300 cal yr BP (AD 1350–1650).

In contrast, gastropods from the auger hole at VEN-6 are notably older (Fig. 9, Table 2). The stratigraphically highest sample, from a depth of 50 cm, returned a radiocarbon age of 2170  $\pm$  30 years. After adjusting for the possible hard-water effect, this result calibrates to ~1750 cal yr BP. A sample (V-6b) obtained from a similar depth in the crest of the lower dune ridge inset to VEN-6 (Fig. 2) returned an age of 2510  $\pm$  15 years. After correction, this result calibrates to

approximately 2140 cal yr BP. Four more samples at depths from 75 to 250 cm in VEN-6 yielded ages that calibrate to between 3140 and 3880 cal yr BP. Finally, the deepest VEN-6 sample, from 300 cm below the surface, yielded a radiocarbon age of  $2880 \pm 15$  years. After correction this age calibrates to approximately 2600 cal yr BP.

#### 5. Discussion

## 5.1. Conditions necessary for Little Lake to form

The combination of data from the Global Surface Water Explorer (GSWE), the Living Blended Drought Atlas (LBDA), the Hole in Mountain SNOTEL station, and climate records for northeastern Nevada clearly indicates that Little Lake forms in years of aboveaverage water availability. Specifically, permanent, seasonal, or no water at Little Lake is highly correlated with snowpack in the East Humboldt Mountains. This result is intuitive, and in of itself is not particularly surprising. However the strong correlation reinforces the degree to which Little Lake, a tiny terminal lake basin many kilometers removed from the mountains, records hydroclimate conditions at higher elevations with high fidelity. Given that these mountains are water towers (Viviroli et al., 2007; Viviroli and Weingartner, 2008) due to their ability to intercept and collect significant amounts of snow in the winter, Little Lake preserves a record of paleohydrology with regional significance disproportionate to its diminutive size.

Close inspection of the time series for Little Lake occurrence and the assembled climate data reveals the suggestion of a lag between peak effective moisture and the presence of water (Fig. 5). For

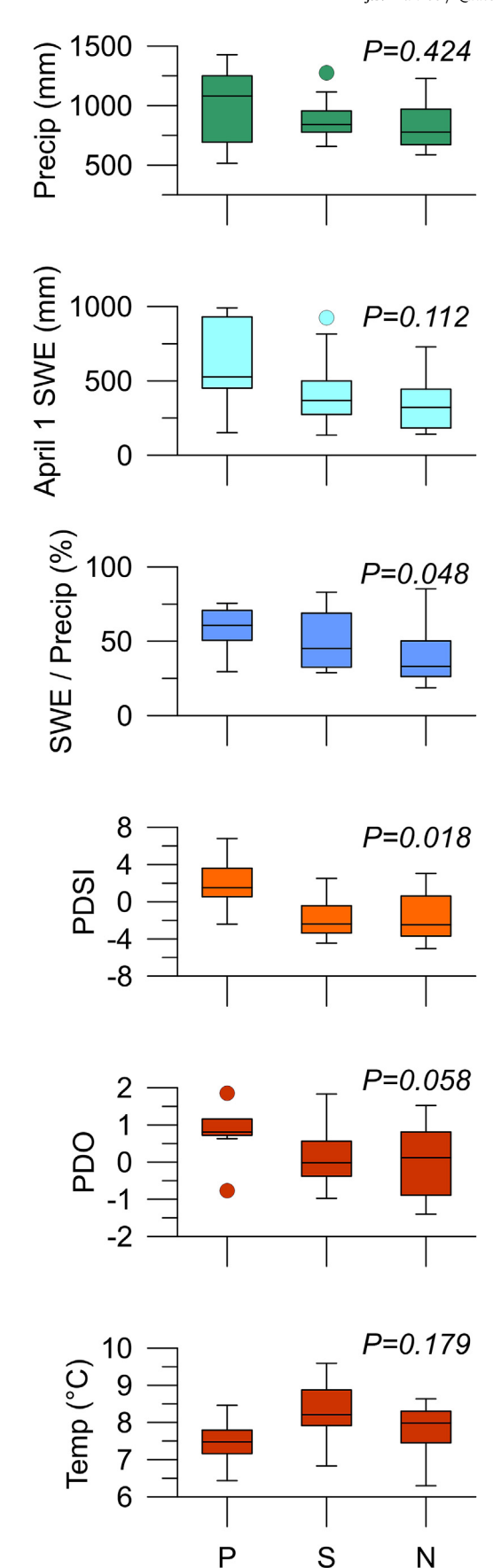


Fig. 6. Box plots presenting climatic data for the region surrounding Little Lake in years of permanent (P), seasonal (S), and no (N) water. Significance values for the

instance, Little Lake was permanent between 1984 and 1987, despite the fact that the PDSI and precipitation were only notably above average in the first year of that interval. Similarly, although the PDSI rose markedly above average in 1995, permanent water at Little Lake was not observed until 1997. This pattern also holds for some of the observations of seasonal water, for instance a positive upturn in the PDSI in 2005 was followed by the appearance of water at Little Lake in 2006 (Fig. 5). On the other hand, in some years a permanent version of Little Lake formed essentially synchronous with peak precipitation, such as in 2017.

The lack of perfect consistency between the timing of increased effective moisture and the appearance of water at Little Lake could reflect a number of natural factors, including the pre-existing moisture deficit in the soil, the rate of snowpack melting in the spring, and differences in summer temperature and average wind speed that impact evaporation. Artificial diversion of water for irrigation and other uses upstream from Little Lake may also obscure a pure climate signal in the water occurrence data set. However, records held by the Nevada Division of Water Resources <a href="http://water.nv.gov/waterrights.aspx">http://water.nv.gov/waterrights.aspx</a> indicate that the only significant change in permitted water diversions upstream of Little Lake during the time period considered here occurred in 1989, in the middle of the sustained interval in which Little Lake was absent, and several years before the lake reappeared in 1997. Thus, although the potential impact of upstream diversions on this system cannot be ruled out, it seems unlikely that diversions alone can entirely explain the observed presence or absence of water on the Little Lake playa. Finally, the database of satellite photos contained within the GSWE is not complete, and although most years have five or more months in which satellite observations of the Little Lake area are available, a few years have less than that (Table 1). This incompleteness raises the possibility that the short-lived presence of water at Little Lake may have been missed in some years, leading to an underestimation of the number of years in which the water occurrence is classified as seasonal. This effect would not have impacted the number of years in which water was described as permanent however.

## 5.2. Sedimentology

Little Lake receives sediment from a number of drainages descending from the East Humboldt Mountains and Wood Hills that feed a single stream crossing the floor of the Clover Valley into the Independence Valley (Fig. 1). Despite the distance separating the lake basin from its headwaters, this rather linear hydrologic system creates an efficient situation for the transport of sediment. As a result, clastic material arriving at Little Lake reflects a wellmixed blend of material from the headwaters. This consistency is clearly seen in the mineralogical and geochemical similarity of samples collected from the two dune crests. The dominance of Si and Ca in this material, combined with the abundance of quartz, calcite, and plagioclase, reflects the presence of gneissic bedrock in the East Humboldt Mountains, as well as carbonate lithologies along the lower flank of the East Humboldt Mountains and in the Wood Hills (Camilleri, 2010; McGrew, 2018). An identical geochemical and mineralogical composition was reported for the dunes at Snow Water Lake (Fig. 1), which also receives sediment from the East Humboldt Mountains (Munroe et al., 2017).

In comparison with other dunes reported in the literature (Muhs, 2004) the sediment comprising the Little Lake dunes is

differences between these three categories were determined with a nonparametric Kruskal Wallis test. The tendency of Little Lake to be permanent during wetter years is clear.

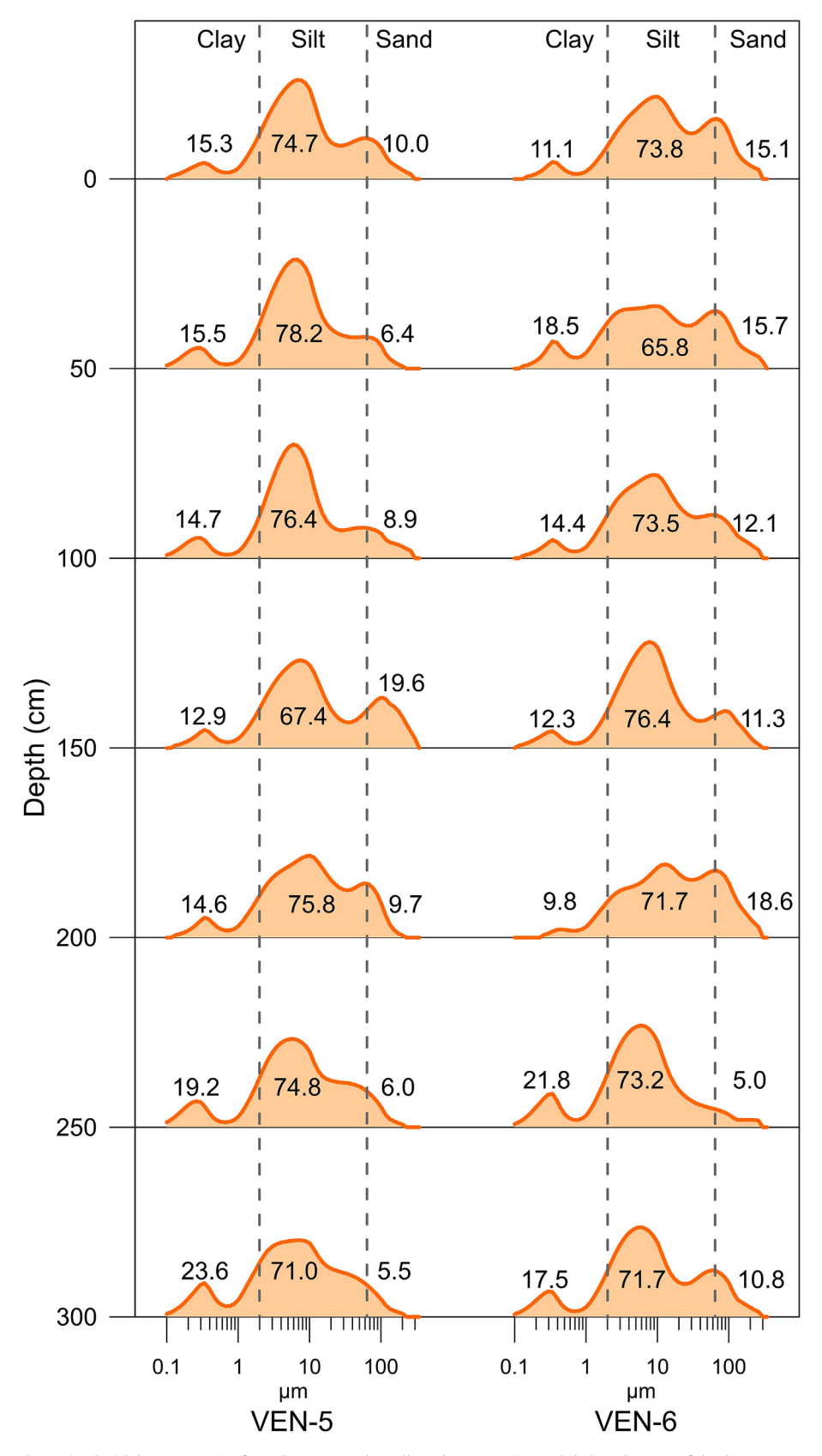
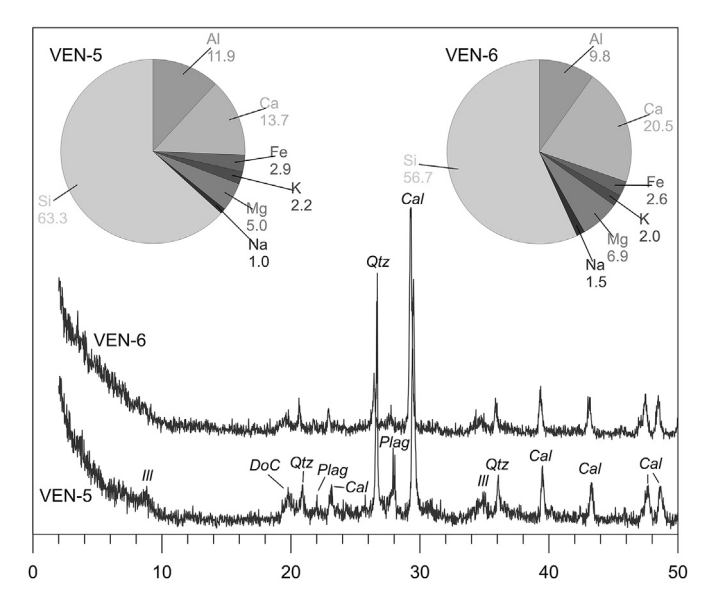


Fig. 7. Grain size distributions determined with laser scattering for sediment samples collected at 50-cm intervals below the crest of the dune at VEN-5 and VEN-6. The abundances of clay ( $<2 \mu m$ ), silt ( $2-63 \mu m$ ), and sand ( $>63 \mu m$ ) in the samples are also shown as percent of the total sample volume. Samples are notably consistent from top to bottom within each auger hole, and between the two dunes, indicating long-term stability of the sedimentary system at this site.



**Fig. 8.** Pie charts presenting the average abundance of major elements (in atomic values) determined with XRF analysis of samples from the VEN-5 and VEN-6 dunes. The abundances of Mn, P, and Ti were ≪1 and were not plotted for clarity. At the bottom, average X-ray diffraction patterns for the VEN-5 and VEN-6 dunes reveal that these sediments are dominated by quartz (Qtz), calcite (Cal), and plagioclase (Plag), with detectable amounts of illite (III) and other dioctahedral clays (DoC). There is no difference in the mineralogical composition of the sediments at the two sites.

mineralogically immature. Measured abundances of SiO<sub>2</sub> average ~60%, whereas the sum of K<sub>2</sub>O, Na<sub>2</sub>O, and Al<sub>2</sub>O<sub>3</sub> averages 14%. In contrast, mineralogically mature dunes usually have SiO<sub>2</sub> contents in excess of 90% and lower feldspar abundances (Muhs, 2004). Because chemical weathering generally eliminates feldspars over time, and concentrates quartz, dunes with immature mineralogies

are typically either young, or are comprised of sediments that have not traveled far from their original source. Both of these criteria apply in the case of the dunes at Little Lake.

The consistent grain size distribution of the Little Lake dunes reflects sorting during fluvial transport away from the mountains, as well as additional eolian sorting in the process of deflating and transporting material from the plava surface to the growing dune crest. The fact that the grain size distributions of this sediment do not appreciably vary with depth in the auger holes (Fig. 7) indicates that the energy available in this sedimentary system has not fluctuated dramatically over time. The tendency for material at the VEN-5 dune to be finer than that at VEN-6 may reflect the fact that the VEN-5 playa is located downstream from VEN-6. Support for this explanation is provided by the grain size distribution of the sediment yielding the gastropod shells at L-7. This material, located at the ultimate downstream end of the drainage system (Fig. 2), has a median grain size of 4.5  $\mu$ m, finer than VEN-6 (8.8  $\mu$ m) or VEN-5 (7.0 µm). Overall, the dunes at Little Lake have an average abundance of sand, silt, and clay that is nearly identical to that reported for the dunes at Snow Water Lake by Munroe et al. (2017), consistent with their formation in a similar system.

## 5.3. Geochronology and hydrologic history

The strong clustering of calibrated radiocarbon ages for samples collected from the Little Lake playa (Table 2, Fig. 9) indicates that it has been 300–400 years since there was an established aquatic gastropod assemblage at this site. Obviously the satellite data and aerial or imagery indicate that Little Lake can exist under the modern climate during years with above-average effective moisture. However, the lack of modern gastropods encountered at Little Lake, or in the kilometers of channel surveyed upstream, combined with the lack of shells reporting ages younger than 600 <sup>14</sup>C years (uncorrected), is a strong indication that a truly permanent lake has

 Table 2

 Radiocarbon results for samples from little lake.

Sample	Accession #	Lab	Depth cm	14C Age <sup>a</sup> yrs	Age Err yrs	Cal Range years BP (probability)		Water Corrected Cal Range years BP (probability)	Median yrs BP	Difference <sup>b</sup> yrs
Slough-19	19Wa/ 0964	ICA	_	360	30	500-420 (47.7%), 410-310 (47.7%)	410	_	-	-
L-7-2019	19S/0468	ICA	0	700	30	<b>690–640 (77.5)</b> , 590–560 (17.9%)	660	490-310 (95.4%)	390	270
VEN-5- playa	19S/0466	ICA	0	680	30	<b>680–630 (60.4%)</b> , 600–560 (35.0%)	650	470-300 (95.4%)	390	260
VEN-5 pit	18S/1120	ICA	50	610	30	660-540 (95.4)	600	430-360 (15.0%), <b>330-270 (55.2%)</b> , 190-140 (21.3%0, 20-0 (4.0%)	300	300
V-5-130	OS-149654	NOSAMS	130	785	15	730-680 (95.4%)	700	520-470 (95.4%)	500	200
V-5-175	OS-149655	NOSAMS	175	900	20	910-740 (95.4%)	840	630-600 (17.6%), <b>560-510 (77.8%)</b>	540	300
V-5-200	OS-149657	NOSAMS	200	860	15	790-730 (95.4%)	760	540-510 (95.4%)	520	240
V-5-250	OS-149658	NOSAMS	250	835	15	790-700 (95.4%)	740	530-500 (95.4%)	520	220
V-5-300	OS-149659	NOSAMS	300	930	15	920-790 (95.4%)	850	<b>640–590 (56.1%)</b> , 570–530 (39.3%)	610	240
VEN-6- playa	18S/1121	ICA	0	650	30	670-620 (43.5%), <b>610–550 (51.9%)</b>	600	460-280 (95.4%)	380	220
VEN-6-pit	19S/0467	ICA	50	2170	30	<b>2310–2100 (92.6%)</b> , 2090–2060 (2.5%)	2210	<b>1830–1690 (86.6%)</b> , 1670–1620 (8.8%)	1750	460
V-6b	OS-149662	NOSAMS	~50	2510	15	2730-2680 (21.9%), 2640-2610 (16.3%), <b>2600-2490 (57.1%)</b>	2580	2300-2250 (23.8%), <b>2160–2100</b> ( <b>67.7%</b> ), 2090–2060 (3.9%)	2140	440
V-6-75	OS-149660	NOSAMS	75	3330	20	3640-3480 (95.4%)	3570	3210-3070 (95.4%)	3140	430
V-6-150	OS-149729	NOSAMS	150	3360	20	3680-3660 (3.0%), <b>3650-3560 (92.4%)</b>	3600	3320-3300 (1.7%), <b>3250-3070 (93.6%</b> )	3190	410
V-6-200	OS-149730	NOSAMS	200	3640	15	4070-4040 (3.3%), <b>3990-3890 (92.1%)</b>	3950	3570-3460 (95.4%)	3510	440
V-6-250	OS-149731	NOSAMS	250	3940	20	4500-4480 (2.6%), <b>4440-4290 (92.8%)</b>	4410	3960-3940 (3.8%), <b>3930-3830 (91.6%</b> )	3880	530
V-6-300	OS-149661	NOSAMS	300	2880	15	3070-2950 (95.4%)	3000	2740-2690 (32.0%), 2640-2610 (16.2%), <b>2600-2500 (47.2%)</b>	2620	380

 $<sup>^{\</sup>rm a}$  Corrected for fractionation using unreported  $\delta^{13}C$  values measured on the accelerator.

<sup>&</sup>lt;sup>b</sup> Shift in median of calibrated age range resulting from subtraction of the water age.

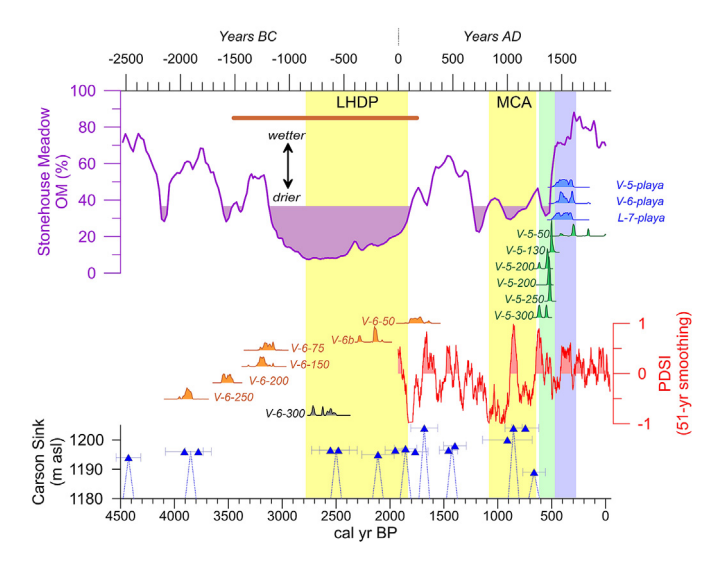


Fig. 9. A composite of radiocarbon results for Little Lake and paleoclimate data for the region. All radiocarbon ages were corrected for a possible hard-water effect as discussed in the text, and calibrated to calendar years with the IntCal13 calibration curve. Three samples from the playa surface (shown in blue), as well as the sample from 50 cm in the VEN-5 dune (green) yield ages from 300 to 400 cal yr BP. Gastropod shells from deeper in the VEN-5 dune (green) yield a group of older ages ~600 cal yr BP. Both of these clusters align with periods of extreme wetness seen in the reconstructed PDSI time-series (red) from the Living Blended Drought Atlas (Cook et al., 2010) and with wetter conditions inferred from total organic matter (purple) in a record from Stonehouse Meadow (Mensing et al., 2013). The older of these intervals also aligns with a dated episode of high water in the Carson Sink (blue triangle), which is fed by the Humboldt River draining from the East Humboldt Mountains (Adams and Rhodes, 2019). Radiocarbon ages from the VEN-6 dune (orange) are older, spanning the interval from 3800 to 1750 cal yr BP; many fall during an interval of low water at Favre Lake (brown bar) inferred from diatoms (Wahl et al., 2015), and several align with episodes of high water in the Carson Sink (triangles). The basal age from VEN-6 is stratigraphically inconsistent and likely represents material that fell down inside the auger hole. The purple and green shading emphasize the two most recent clusters of radiocarbon ages. The areas of yellow shading delineate the Medieval Climate Anomaly-MCA (Stine, 1994) and the Late Holocene Dry Period-LHDP (Mensing et al.,

not existed at this site for several centuries.

Furthermore, the projectile point noted on the playa surface at VEN-6 (Fig. 4) appears to be a Rosegate Series point, resembling the Eastgate Expanding Stem type (Smith et al., 2013; Thomas, 1981). The Rosegate Series dates to 650–1250 cal yr BP (AD 700 to AD 1300) making it somewhat older than the calibrated <sup>14</sup>C ages for the shells on the playa surface (which average AD 1560). However some studies have suggested that Rosegate points span a wider time range extending to younger ages (Oetting, 1994; Schmitt and Madsen, 2005). Given that the playa is deflating, it is also possible that the point was originally emplaced at a stratigraphic level deeper (older) than the shells collected and dated from the current playa surface. Either way, the presence of this point is consistent with a situation in which permanent water at Little Lake was attractive to waterfowl and other large animals, and to the people who hunted them (Holliday et al., 2019).

The youngest radiocarbon age from a depth of 50 cm beneath the crest of the VEN-5 dune overlaps on the younger end of the calibrated age ranges for shells from the playa surface (Fig. 9). It seems likely therefore, that the most recent addition of sediment to this dune occurred in response to the desiccation of a formerly permanent Little Lake sometime after 300 cal yr BP.

In contrast, samples from deeper beneath the crest of this dune (130–300 cm) form a cluster of older ages that does not overlap with the samples from the playa and the VEN-5 crest (Fig. 9). The 4 samples between 130 and 250 cm have calibrated age ranges with

median probabilities that align at 520 cal yr BP. The sample from 300 cm is slightly older, with a median 610 cal yr BP, however a considerable part of the calibrated age range for the sample does overlap with the four samples stratigraphically above it. Collectively, this set of ages indicates that most of the upper 3 m of the VEN-5 dune accumulated around 520 cal yr BP, approximately 130 years before the uppermost sediment and the shells on the surface of the playa. This convergence suggests that the dune at VEN-5 grew quite rapidly in response to a single desiccation event.

The fact that the playa ages (ca. 390 cal yr BP) and nearly all of the ages from VEN-5 (ca. 520 cal yr BP), form two non-overlapping clusters is significant. The best interpretation of this pattern is that there were two intervals of persistent lake conditions, each long enough to allow establishment of a robust gastropod fauna. The first of these occurred in the decades before 520 cal yr BP and ended with the desiccation event ca. 520 cal yr BP. The second occurred in the decades before ca. 390 cal yr BP, may have lasted until 300 cal yr BP (or later) and was also followed by a desiccation event that fostered dune growth.

The radiocarbon ages from the VEN-6 dune tell a very different story. With the exception of the deepest sample at 300 cm – which can be explained as the unfortunate outcome of stratigraphically higher sediment falling down inside the deep auger hole - the radiocarbon ages are in stratigraphic order with median calibrated values ranging from 1750 to 3880 cal yr BP (Fig. 9). This contrast with the ages from VEN-5 is striking, particularly given the similarity of the sediment comprising these dunes in terms of grain size, geochemistry, and mineralogy (Figs. 7 and 8). The best interpretation of the available evidence is that the VEN-6 was constructed by the same processes as VEN-5, but is in actuality several thousand years older. Furthermore, the VEN-6 dune is not just older than VEN-5, it was apparently built over a much longer interval of time (Fig. 9). Although deflation of sediment from the playa surface and delivery to the dune is unlikely to be a steady process, calculating an average sedimentation rate is illustrative: the 250 cm of sediment between the deepest (610 cal yr BP) and shallowest (300 cal yr BP) samples at VEN-5 accumulated at a rate of 8 mm/yr, as opposed to 0.9 mm/yr for the sediment between the 250-cm sample (3880 cal yr BP) and the 50-cm sample (1750 cal yr BP) at VEN-6. An additional consideration is the fact that the dated samples (excepting the deepest one) are in chronostratigraphic order (Fig. 9). This would not be the case if a thick package of lake sediment was slowly deflated and recompiled as a dune; that scenario would result in an inverted stratigraphy of older radiocarbon ages near the dune crest, reflecting sediment that was originally deeper in the lake basin fill. It seems likely, therefore that the dune at VEN-6 accumulated as a result of multiple lake filling and desiccation events over ~2000 years. For comparison, the two separate desiccation events apparently recorded by the bulk of the VEN-5 dune and the dune crest/playa surface ages indicate that lake formation and establishment of a preservable gastropod fauna can occur in a century or less. Thus, there was enough time between each of the ages in the VEN-6 dune for this cycle to have been repeated multiple times.

The two small basins that together form Little Lake (Fig. 2) are connected by a short channel that wraps around the northern end of the VEN-6 dune. This arrangement, combined with the lack of overlap between the radiocarbon ages from the VEN-6 (older) and VEN-5 (younger) dunes suggests that the upstream basin at VEN-6 was the termination for the drainage system leading to Little Lake during at least the interval from ~4000 to 1750 cal yr BP. At some point before ~600 cal yr BP (the age of the deepest dated sample from VEN-5) Little Lake must have grown large enough to overflow around the end of the VEN-6 dune, forming the short channel and creating the new terminal basin at VEN-5. After this point, most

water and sediment could bypass the VEN-6 basin and travel directly downstream to VEN-5. Observations of inundation patterns at Little Lake (Fig. 3) reveal that substantial parts of the VEN-6 playa remain dry when the downstream playa is completely flooded. Given that the radiocarbon dates for shells from the two playa surfaces are essentially identical (Table 2), it is clear that at certain times both are perennially inundated. However, a shift of the primary depocenter from VEN-6 two VEN-5 in the late Holocene would explain the lack of overlap between the ages from the two dunes.

Overall, the available evidence suggests that Little Lake formed at the location of VEN-6 multiple times between ~4000 and 1750 cal yr BP. Each time, after persisting long enough to allow a gastropod fauna to become established (likely several decades), the lake desiccated in response to a negative shift in effective moisture. Sediment (including shells) was then deflated from the lake bed and added incrementally to the lunette. At some point in the late Holocene, Little Lake grew large enough to flood northward around the lunette at VEN-6, which had come to serve as a dam. This outflow carved a short channel leading to a new basin, VEN-5, and the Little Lake system expanded to encompass two interconnected playas. Water and sediment began to partially bypass the upstream basin, although the radiocarbon date from the VEN-6 playa indicates that both basins were occasionally inundated. At least twice in the late Holocene, Little Lake again persisted long enough to become colonized by gastropods. Once again, each of these episodes of permanent water was followed by a desiccation event that led to growth of the new lunette at VEN-5. Minor overflow from this basin also extended northward to the location of sample L-7 (Fig. 2). The last episode of truly perennial water in the Little Lake system ended before 300 cal yr BP. Since that time, although the lake has re-formed at times in response to particularly wet conditions in the East Humboldt Mountains, the lake has not persisted for long enough to permit the return of aquatic snails.

## 5.4. Paleoclimate implications

The combination of observational data from the GSWE and climate data from the past few decades constrains the conditions under which Little Lake forms, and the radiocarbon data permit construction of hydroclimate chronology extending back several thousand years. At the simplest level, the lack of shells collected at the Little Lake study site having corrected, calibrated radiocarbon ages younger than 300 cal yr BP indicates that conditions have been too dry in this area over the last several centuries for Little Lake to persist for more than a few years at a time. In contrast, between roughly 600 and 300 cal yr BP, the situation was different and Little Lake existed long enough in (at least) two separate intervals to become colonized by aquatic gastropods. The presence of a projectile point on the modern playa surface (Fig. 4) in association with shells dating to approximately 400 cal yr BP is additional indirect evidence that a productive ecosystem with perennial water was present at Little Lake at this time.

Comparison of the groupings of radiocarbon ages from the playa surface and the VEN-5 dune with the estimated PDSI values for the LBDA grid point closest to Little Lake (Fig. 1) reveals that both clusters of radiocarbon ages align with intervals of notably elevated effective moisture, separated by a multi-decadal drought (Fig. 9). The magnitude of these wet periods at this particular node in the LBDA exceeds anything that occurred in the centuries since the youngest radiocarbon-constrained lake desiccation event, which is consistent with the apparent lack of a truly permanent lake at this location since roughly 300 cal yr BP. A similar pattern is seen in a time series of organic matter from Stonehouse Meadow in eastern Nevada (Fig. 1), which exhibits high values (corresponding with

maximum wetness) from 500 to 300 cal yr BP, followed by a shift to drier conditions (Fig. 9; Mensing et al., 2013).

The LBDA also reveals that the ultimate peak of positive PDSI values in the past 2000 years occurred slightly earlier, circa 850 BP. No shells dating to this time were encountered at the VEN-5 site, but sediment of this age could be present below the depth reached by the auger (300 cm). Extremely wet conditions at this time may also have been the reason that Little Lake overflowed its basin at VEN-6, carving the channel leading to VEN-5. On the other hand, it is worth noting that if the radiocarbon ages are not corrected using the water sample, then the two clusters of ages (the playa surface and the majority of the samples from VEN-5) shift slightly older and align with the two most prominent peaks in the reconstructed PDSI at 850 and 600 BP (Table 2). This is an intriguing correlation, but in the absence of other constraints on the potential hard-water effect in this system, it seems prudent to rely more heavily on the corrected ages.

The centuries between AD 850 and 1300 featured notably variable temperature and precipitation conditions and are referred to as the Medieval Climate Anomaly (MCA). None of the corrected radiocarbon ages from Little Lake date to this time interval, which could be indirect evidence that conditions were too dry during the MCA for Little Lake to form. Previous work has identified various signals of the MCA in paleoclimate records from the northern Great Basin (Cook et al., 2016, 2010; Reinemann et al., 2014). Most dramatic are radiocarbon dates from the remains of full-grown trees rooted in the bottoms of Lake Tahoe, Fallen Leaf Lake, and other lakes in the Sierra Nevada (Kleppe et al., 2011; Morgan and Pomerleau, 2012: Stine, 1994), Given their position, these trees could only have grown at times when water level in these lakes was considerably lower, as would be the case in response to prolonged drought. The calibrated radiocarbon ages for these trees extend from roughly AD 1000–1300; subtracting the years of growth from counted tree rings indicates that the MCA began around AD 800 (Kleppe et al., 2011). In some cases, death dates on submerged trees cluster in two discrete intervals, consistent with extreme variations in hydroclimate during the MCA (Stine, 1994). The younger of these two intervals, ca. AD 1300-1400 (Stine, 1994), overlaps with the ages from the VEN-5 dune, suggesting that these trees were drowned by rising water level at the same time the Little Lake formed for its penultimate time.

Another recent study combined tree-ring-based hydrology reconstructions with geochronology to reconstruct the late Holocene hydroclimate history of the Carson Sink and Walker Lake in northern Nevada (Adams and Rhodes, 2019). The results for the Carson Sink are particularly relevant to Little Lake because both receive runoff from the East Humboldt Mountains. Numerous lake highstands in the normally dry Carson Sink were noted, each of which lasted a few decades (Fig. 9). One of these, ca. 600 cal yr BP, overlaps with the majority of the ages from the VEN-5 dune, suggesting a regional increase in effective moisture that elevated water levels in both of these basins simultaneously. Additional episodes of high water in the Carson Sink ca. 1700, 2100, 2500, and 3800 cal yr BP also match calibrated radiocarbon ages from Little Lake (Fig. 9). Collectively this pattern is strong support for the interpretation that the sedimentary record at Little Lake faithfully records regional hydroclimate variability.

An earlier, prolonged episode of drier conditions, known as the Late Holocene Dry Period (LHDP), has been reported for the Great Basin between 2800 and 1850 BP (Mensing et al., 2013). Evidence for this sustained period of aridity has been reported from a variety of sites, including at Favre Lake in the Ruby Mountains (Fig. 1), where conditions were drier between 3450 and 1750 cal yr BP (Wahl et al., 2015) and in the Sierra Nevada where June Lake (Fig. 1) contains evidence of repeated drought between 3600 and

1700 cal yr BP (Lyon et al., 2020). There is a tendency for locations farther to the north to exhibit ambiguous evidence for drought, or even suggestions of wetter conditions at this time (Mensing et al., 2013), with a boundary between 40 and 42° N. Little Lake, and the drainage basin feeding it, are at 41° N (Fig. 1), suggesting that this system was positioned at the tipping point between notably drier and possibly wetter conditions. The uppermost ages from the VEN-6 dune fall within the LHDP, indicating that perennial water was present at Little Lake on at least two occasions during this time interval (Fig. 9). At the same time, studies have noted that the LHDP was characterized by wide amplitude fluctuations in effective moisture (Benson et al., 2002). Thus, it is plausible that conditions during the LHDP were occasionally wet enough to sustain Little Lake, particularly given its location near the northern boundary of the region impacted by this drought. Furthermore, water levels apparently rose in the Carson Sink numerous times during the LHDP (Adams and Rhodes, 2019), and some of these increases correspond with radiocarbon dates from Little Lake (Fig. 9).

A variety of additional paleoclimate records for the latter half of the Holocene from this region have bearing on interpretations of the record from Little Lake. For example, multiproxy investigation of sediment cores from lakes in the East Humboldt and Ruby Mountains indicate that climatic conditions became more variable after 3800 cal yr BP (Munroe et al., 2018). This timing aligns with the episodic growth of the dune at VEN-6 and the eventual formation of the channel leading to the new basin at VEN-5. Also in the Ruby Mountains, diatom evidence from Fayre Lake suggests wetter and more variable conditions after 1750 cal vr BP, spanning the interval in which the VEN-5 dune was constructed (Wahl et al., 2015). At Blue Lake in the Bonneville Basin to the east of Little Lake (Fig. 1), pollen evidence suggests warmer conditions between 3400 and 2700 cal yr BP, and again after 1500 cal yr BP (Louderback and Rhode, 2009), which could have contributed to the impermanence of water at Little Lake. Farther to the east, at least parts of the Great Salt Lake became fresh enough to host moderately salt-tolerant fish at roughly 3400 and 1200 cal yr BP (Madsen et al., 2001). The first of these intervals aligns with radiocarbon ages from the middle part of the auger hole at VEN-6 (Fig. 9), suggesting that conditions were simultaneously wet at both locations. Finally, generally drier conditions interrupted by short-lived, but significant rises in water level characterized Fallen Leaf Lake (Fig. 1) from 3650 until 550 cal yr BP, (Noble et al., 2016), and following a drier interval at June Lake, drought became less frequent after 1700 cal yr BP (Lyon et al., 2020). The intermittent formation/desiccation of Little Lake during the late Holocene is consistent with a similar pattern of punctuated aridity over the last several millennia.

## 5.5. Directions for future work

The results reported here for Little Lake provide valuable insight into late Holocene hydroclimate variability in the northern Great Basin. Nonetheless, these data and their interpretations have limitations that could be addressed by future work. One challenge is the imperfect understanding of the potential hard-water effect in the Little Lake system. Radiocarbon dating of the dissolved inorganic carbon in the stream water, as employed here, is an indirect way of constraining the hard-water effect. Subtraction of this radiocarbon age from the shell ages before calibration is a conservative way to accommodate the fact that the actual death ages for the gastropods are likely younger than their radiocarbon ages. However it is not possible to determine the true magnitude of this offset from the available evidence. Future efforts aimed at the collection and radiocarbon dating of live snails from the Little Lake watershed would be an important step toward better interpretation of the radiocarbon ages from older shells.

Similarly, it would be useful to expand the approach employed here to the other lunettes present to the southeast of Little Lake (Fig. 2). Reconnaissance of these playas and their associated dunes failed to reveal gastropod shells. However, auguring into the dunes might permit the collection of shells from deeper, buried sediment where shells would be less vulnerable to leaching and dissolution. Luminescence analysis is also an option to determine the burial age of the dune sediments if radiocarbon-datable material is not present (Lancaster and Mahan, 2012; Munroe et al., 2017). In terms of their form and position, these playa-dune pairs appear identical to Little Lake. Constraints on their ages, therefore, could extend the hydroclimate record for this system farther back into the Holocene. Auguring beneath the playa surface at Little Lake and the other playas could also be an approach for collecting older shells and sediment.

Finally, geophysical techniques such as ground penetrating radar (GPR) could be used to investigate the internal structure of these dunes and clarify interpretations of how they were constructed (Fu et al., 2019; Hugenholtz et al., 2007). For instance, if the dune at VEN-6 was built by multiple depositional events spaced centuries apart in time, then GPR might be able to detect stratigraphic evidence in the form of paleosols or incipient caliche that was not noticed in the bucket auguring. GPR could also clarify the relationship between the main dune crest at VEN-6 and the inset ridge where the VEN-6b sample was collected (Fig. 2). Depending on the conditions and antenna frequency, GPR may also be able to image sediment at greater stratigraphic depths than can be reached by hand auguring, providing information about the deepest, oldest parts of each dune ridge.

## 6. Conclusion

This research developed a hydroclimate record for the northern part of the Great Basin in southwestern North America from lacustrine and eolian sediments associated with a terminal basin known as Little Lake. The basin receives runoff from the East Humboldt Mountains, which are also the source of the longest river system within the Great Basin, the Humboldt River. The sediments at Little Lake, therefore, serve as a recorder of hydroclimate conditions over an area significantly larger than the lake's watershed. Analysis of remotely sensed data spanning the last several decades revealed specific years in which Little Lake was present. A variety of recent climate data indicate that the accumulation of an unusually deep snowpack in the mountains is necessary for the lake to form. Radiocarbon dating of gastropod shells from the Little Lake playa reveals that a perennial aquatic ecosystem was last present at this site 300-400 cal yr BP. The centuries since then have apparently been too dry to support perennial water for more than a few years at a time, insufficient to allow formation of a preservable gastropod fauna. The presence of Little Lake immediately before ~400 cal vr BP, as well as radiocarbon-dated evidence for an earlier iteration of the lake ~600 cal yr BP, match evidence for wet conditions in this region at those times in a time-series of PDSI values reconstructed from tree-ring data. A dune associated with the upstream basin of Little Lake is notably older, and appears to have formed over a longer period of time between roughly 3800 and 1750 BP, partly overlapping the Late Holocene Dry Period (Mensing et al., 2013). Formation of this dune, with radiocarbon ages in chronostratigraphic order, suggests a long period of varying conditions during which a lake alternately formed, persisted long enough for a gastropod fauna to become established, and then desiccated leading to eolian deflation and dune growth. Overall, the hydrologic record presented here for Little Lake exhibits strong similarities with other paleoclimate records for the northern Great Basin, including a paleohydrological record for the Carson Sink (Adams and Rhodes, 2019) that is also fed by runoff from the East Humboldt Mountains. These results contribute to an emerging and detailed picture of late Holocene climate change in this region, and shed important light on hydroclimate variability in particular. Given the reliance of a growing population on the meager water resources of the Great Basin, better understanding of hydroclimate variability is crucial for making accurate predictions of future water availability.

## **Author statement**

The author, Jeffrey S. Munroe, is solely responsible for all aspects of this project, from conceptualization, methodology and funding; through field and laboratory analysis; to data interpretation and writing.

## **Declaration of competing interest**

The author declares that he has no known competing financial interests or personal relationships that could have appeared to influence the work reported in this paper.

## **Acknowledgments**

Middlebury students Bryce Belanger, Jackson Hawkins, Kira Ratcliffe, and Caleb Walcott contributed to successful fieldwork. Greg Haynes identified the Rosegate Series point. This work was supported by National Science Foundation award P2C2-1702975 to J. Munroe. Scott Mensing kindly provided the data from Stonehouse Meadow. The author appreciates the thoughtful comments of Suzanne Zimmerman and an anonymous reviewer.

#### References

- Adams, K.D., Rhodes, E.J., 2019. Late Holocene paleohydrology of Walker Lake and the Carson Sink in the western Great Basin, Nevada, USA. Quat. Res. 92, 165-182. https://doi.org/10.1017/qua.2018.151.
- Adams, K.D., Wesnousky, S.G., 1998. Shoreline processes and the age of The lake lahontan highstand in the jessup embayment, Nevada. Geol. Soc. Am. Bull. 110, 1318-1332. https://doi.org/10.1130/0016-7606(1998)110<1318: SPATAO>2.3.CO;2.
- Bacon, S.N., Burke, R.M., Pezzopane, S.K., Jayko, A.S., 2006. Last glacial maximum and Holocene lake levels of Owens Lake, eastern California, USA. Quat. Sci. Rev. 25, 1264-1282. https://doi.org/10.1016/j.quascirev.2005.10.014.
- Benson, L., Kashgarian, M., Rye, R.O., Lund, S.P., Paillet, F.L., Smoot, I.P., Kester, C.L., Mensing, S., Meko, D., Lindstrom, S., 2002. Holocene multidecadal and multicentennial droughts affecting Northern California and Nevada, Ouat, Sci. Rev. 21. 659-682.
- Benson, L.V., Lund, S.P., Smoot, J.P., Rhode, D.E., Spencer, R.J., Verosub, K.L., Louderback, L.A., Johnson, C.A., Rye, R.O., Negrini, R.M., 2011. The rise and fall of Lake Bonneville between 45 and 10.5 ka. Quat. Int. 235, 57-69. https://doi.org/ 10.1016/i.guaint.2010.12.014.
- Benson, L.V., Paillet, F.L., 1989. The use of total lake-surface area as an indicator of climatic change; examples from the Lahontan Basin. Quatern.Res. 32, 262-275. Camilleri, P., 2010. Geologic Map of the Wood Hills, Elko County, Nevada. Map. 172.
- Cayan, D.R., Das, T., Pierce, D.W., Barnett, T.P., Tyree, M., Gershunov, A., 2010. Future dryness in the southwest US and the hydrology of the early 21st century drought. Proc. Natl. Acad. Sci. Unit. States Am. 107, 21271–21276.
- Cook, B.I., Cook, E.R., Smerdon, J.E., Seager, R., Williams, A.P., Coats, S., Stahle, D.W., Díaz, J.V., 2016. North American megadroughts in the common era: reconstructions and simulations. Wiley Interdisciplinary Reviews: Climate Change 7, 411-432.
- Cook, E.R., Seager, R., Heim Jr., R.R., Vose, R.S., Herweijer, C., Woodhouse, C., 2010. Megadroughts in North America: placing IPCC projections of hydroclimatic change in a long-term palaeoclimate context. J. Quat. Sci. 25, 48-61.
- Frey, W.H., 2012. Population Growth in Metro America since 1980. The Brookings Institution, mars.
- Fu, T., Wu, Y., Tan, L., Li, D., Wen, Y., 2019. Imaging the structure and reconstructing the development of a barchan dune using ground-penetrating radar. Geomorphology 341, 192-202.
- Grayson, D., 2011. The Great Basin: a Natural History. Hatchett, B.J., Boyle, D.P., Putnam, A.E., Bassett, S.D., 2015. Placing the 2012–2015 California-Nevada drought into a paleoclimatic context: insights from Walker Lake, California-Nevada, USA. Geophys. Res. Lett. 42, 8632-8640.
- Held, I.M., Soden, B.J., 2006. Robust responses of the hydrological cycle to global warming. J. Clim. 19, 5686-5699. https://doi.org/10.1175/JCLI3990.1.

- Holliday, V.T., Harvey, A., Cuba, M.T., Weber, A.M., 2019. Paleoindians, paleolakes and paleoplayas: landscape geoarchaeology of the tularosa basin, New Mexico. Geomorphology, Human Geomorphological Interactions and the Legacy of Karl Butzer 331, 92–106. https://doi.org/10.1016/j.geomorph.2018.08.012.
- Hugenholtz, C.H., Moorman, B.J., Wolfe, S.A., 2007. Ground penetrating radar (GPR) imaging of the internal structure of an active parabolic sand dune. Spec. Pap. Geol. Soc. Am. 432, 35.
- Karl, T.R., Melillo, J.M., 2009. Global Climate Change Impacts in the United States. Cambridge Univ Press
- Kleppe, J.A., Brothers, D.S., Kent, G.M., Biondi, F., Jensen, S., Driscoll, N.W., 2011. Duration and severity of medieval drought in The lake Tahoe basin, Quat. Sci. Rev. 30, 3269-3279.
- Laabs, B.J., Munroe, J.S., Best, L.C., Caffee, M.W., 2013. Timing of the last glaciation and subsequent deglaciation in the Ruby mountains, Great Basin, USA. Earth Planet Sci. Lett. 361, 16-25.
- Lancaster, N., Mahan, S.A., 2012. Holocene dune formation at ash meadows national wildlife area, Nevada, USA. Quatern.Res. 78, 266-274.
- Long, S.P., 2019. Geometry and magnitude of extension in the Basin and Range Province (39 N), Utah, Nevada, and California, USA: constraints from a provincescale cross section. Bulletin 131, 99-119.
- Louderback, L.A., Rhode, D.E., 2009. 15,000 Years of vegetation change in the Bonneville basin; the Blue Lake pollen record; Special theme; modern analogues in Quaternary palaeoglaciological reconstruction. In: XVII INQUA Congress Special Session, Cairns, AUS, Australia, 2007, vol. 28, pp. 181–260. https://doi.org/10.1016/j.quascirev.2008.09.027, 308–326.
- Lyon, E.C., McGlue, M.M., Erhardt, A.M., Kim, S.L., Stone, J.R., Zimmerman, S.R.H., 2020. Late Holocene hydroclimate changes in the eastern Sierra Nevada revealed by a 4600-year paleoproduction record from June Lake, CA. Quat. Sci. Rev. 242, 106432. https://doi.org/10.1016/j.quascirev.2020.106432.
- Madsen, D.B., Rhode, D., Grayson, D.K., Broughton, J.M., Livingston, S.D., Hunt, J., Quade, J., Schmitt, D.N., Shaver III, M.W., 2001. Late quaternary environmental change in the Bonneville Basin, western USA. Palaeogeogr. Palaeoclimatol. Palaeoecol. 167, 243-271.
- McGrew, A.J., 2018. Geologic Map of the Humboldt Peak Quadrangle, Elko County, Nevada, Map. 186.
- Mensing, S.A., Sharpe, S.E., Tunno, I., Sada, D.W., Thomas, J.M., Starratt, S., Smith, J., 2013. The Late Holocene Dry Period: multiproxy evidence for an extended drought between 2800 and 1850 cal yr BP across the central Great Basin, USA. Quat. Sci. Rev. 78, 266–282. https://doi.org/10.1016/j.quascirev.2013.08.010.
- Mifflin, M.D., Wheat, M.M., 1979. Pluvial Lakes and Estimated Pluvial Climates of Nevada. Nevada Bureau of Mines and Geology.
- Morgan, C., Pomerleau, M.M., 2012. New evidence for extreme and persistent terminal medieval drought in California's Sierra Nevada. J. Paleolimnol. 47, 707-713.
- Muhs, D.R., 2004. Mineralogical maturity in dunefields of north America, africa and Australia. Geomorphology 59, 247-269.
- Munroe, J.S., Bigl, M.F., Silverman, A.E., Laabs, B.J., 2018. Records of late quaternary environmental change from high-elevation lakes in the Ruby mountains and East Humboldt range, Nevada. In: Starratt, S.W., Rosen, Michael R. (Eds.), From Saline to Freshwater: the Diversity of Western Lakes in Space and Time. Geological Society of America. Geological Society of America Special Paper 536.
- Munroe, J.S., Gorin, A.L., Stone, N.N., Amidon, W.H., 2017. Properties, age, and significance of dunes near snow water lake, Elko County, Nevada. Quat. Res. 87,
- Munroe, J.S., Laabs, B.J., 2013a. Latest Pleistocene history of pluvial lake franklin, northeastern Nevada, USA. Geol. Soc. Am. Bull. 125, 322-342.
- Munroe, J.S., Laabs, B.J., 2013b. Temporal correspondence between pluvial lake highstands in the southwestern US and Heinrich Event 1. J. Quat. Sci. 28, 49-58.
- Munroe, J.S., Walcott, C.K., Amidon, W.H., Landis, J.D., 2020. A top-to-bottom luminescence-based chronology for the post-LGM regression of a Great Basin pluvial Lake. Quaternary 3, 11. https://doi.org/10.3390/quat3020011.
- Noble, P.J., Ball, G.I., Zimmerman, S.H., Maloney, J., Smith, S.B., Kent, G., Adams, K.D., Karlin, R.E., Driscoll, N., 2016. Holocene paleoclimate history of Fallen Leaf Lake, CA., from geochemistry and sedimentology of well-dated sediment cores. Quat. Sci. Rev. 131 (Part A), 193-210. https://doi.org/10.1016/j.quascirev.2015.10.037.
- Oetting, A.C., 1994. Chronology and time markers in the northwestern Great Basin: the Chewaucan basin cultural chronology. In: Aikens, C.M., Jenkins, D.L. (Eds.), Archaeological Researches in the Northern Great Basin: Fort Rock Archaeology since Cressman. Anthropological Papers, p. 50.
- Poage, M., Chamberlain, C., 2002. Stable isotopic evidence for a pre-Middle Miocene rain shadow in the western Basin and Range: implications for the paleotopography of the Sierra Nevada. Tectonics 21, 16-21-16-10.
- Ramsey, C.B., 2006. Development of the radiocarbon calibration program Oxcal. Radiocarbon 43, 355-363.
- Reheis, M., 1999a. Extent of Pleistocene Lakes in the Western Great Basin (Miscellaneous Field Studies Map-U. S. Geological Survey, Report: MF-2323). U. S. Geological Survey, Reston, VA, United States (USA), United States (USA).
- Reheis, M., 1999b. Highest pluvial-lake shorelines and Pleistocene climate of the western Great Basin. Quatern.Res. 52, 196-205. https://doi.org/10.1006/ gres.1999.2064.
- Reimer, P.J., Bard, E., Bayliss, A., Beck, J.W., Blackwell, P.G., Ramsey, C.B., Buck, C.E., Cheng, H., Edwards, R.L., Friedrich, M., others, 2013. IntCal13 and Marine13 radiocarbon age calibration curves 0-50,000 years cal BP. Radiocarbon 55,
- Reinemann, S.A., Porinchu, D.F., Bloom, A.M., Mark, B.G., Box, J.E., 2009. A multi-

- proxy paleolimnological reconstruction of Holocene climate conditions in the Great Basin, United States. Quatern.Res. 72, 347—358. https://doi.org/10.1016/j.yqres.2009.06.003.
- Reinemann, S.A., Porinchu, D.F., MacDonald, G.M., Mark, B.G., DeGrand, J.Q., 2014. A 2000-yr reconstruction of air temperature in the Great Basin of the United States with specific reference to the Medieval Climatic Anomaly. Quat. Res. 82, 309—317
- Salzer, M.W., Bunn, A.G., Graham, N.E., Hughes, M.K., 2014. Five millennia of paleotemperature from tree-rings in the Great Basin, USA. Clim. Dynam. 42, 1517–1526
- Schmitt, D.N., Madsen, D.B., 2005. Camels Back Cave. University of Utah Press.
- Sharp, R.P., 1938. Pleistocene glaciation in the Ruby-East Humboldt range, northeastern Nevada with abstract in German by kurt E. Lowenstein. Journal of Geomorphology 1, 296–323.
- Smith, G.M., Barker, P., Hattori, E.M., Raymond, A., Goebel, T., 2013. Points in time: direct radiocarbon dates on Great Basin projectile points. Am. Antiq. 78, 580–594.
- Steponaitis, E., Andrews, A., McGee, D., Quade, J., Hsieh, Y.-T., Broecker, W.S., Shuman, B.N., Burns, S.J., Cheng, H., 2015. Mid-Holocene drying of the US Great Basin recorded in Nevada speleothems. Quat. Sci. Rev. 127, 174–185.

- Stine, S., 1994. Extreme and persistent drought in California and Patagonia during mediaeval time. Nature 369, 546–549.
- Thomas, D.H., 1981. How to classify the projectile points from Monitor Valley, Nevada. J. Calif. Great Basin Anthropol. 3, 7–43.
- Viviroli, D., Dürr, H.H., Messerli, B., Meybeck, M., Weingartner, R., 2007. Mountains of the world, water towers for humanity: typology, mapping, and global significance. Water Resour, Res. 43.
- Viviroli, D., Weingartner, R., 2008. "Water towers"—a global view of the hydrological importance of mountains. In: Mountains: Sources of Water, Sources of Knowledge. Springer, pp. 15–20.
- Wahl, D., Starratt, S., Anderson, L., Kusler, J., Fuller, C., Addison, J., Wan, E., 2015. Holocene environmental changes inferred from biological and sedimentological proxies in a high elevation Great Basin lake in the northern Ruby Mountains, Nevada, USA. In: Proceedings of the 26th Pacific Climate Workshop, vol. 387, pp. 87–98. https://doi.org/10.1016/j.quaint.2015.03.026.
- Wiens, J.A., Patten, D.T., Botkin, D.B., 1993. Assessing ecological impact assessment: lessons from Mono Lake, California. Ecol. Appl. 3, 595–609. Zimmerman, S.R., Hemming, S.R., Hemming, N.G., Tomascak, P.B., Pearl, C., 2011.
- Zimmerman, S.R., Hemming, S.R., Hemming, N.G., Tomascak, P.B., Pearl, C., 2011. High-resolution chemostratigraphic record of late Pleistocene lake-level variability, Mono Lake, California. GSA Bulletin 123, 2320—2334.